coatings

MDPI

Article

Performance and Thermal Properties of 3D Printed CF-Reinforced PLA Monofilaments

Pen Jin [1,2,3,*], Tuo Pan [1], Yaxuan Li [1], Tianran Zhong [1], Jing Jiang [1], Chengcui Pu [1] and Chunyang Ma [3]

[1] College of Chemical Engineering and Technology, Northwest Minzu University, Lanzhou 730000, China; 2256260499@163.com (T.P.); 2657287448@163.com (Y.L.); 2220375939@163.com (T.Z.); 2509899811@163.com (J.J.); chengcuipu123@163.com (C.P.)
[2] Key Laboratory of Environment-Friendly Composite Materials of the State Ethnic Affairs Commission, Lanzhou 730000, China
[3] Gansu Provincial Biomass Function Composites Engineering Research Center, Lanzhou 730000, China; chunyangandma1@163.com
* Correspondence: 186132287@xbmu.edu.cn

Abstract: This study reports the fabrication of carbon fiber-reinforced poly(lactic acid) (CF-PLA) monofilaments using 3D printing technology. The effects of print head movement speed and retraction rate on the diameter of the CF-PLA monofilaments were investigated. The surface morphology and properties were analyzed using scanning electron microscopy (SEM) and thermogravimetric analysis (TGA). The CF-PLA monofilaments were also printed into boards with varying CF content, and the mechanical properties of these boards were assessed. The results showed that the optimal printing parameters were a nozzle diameter of ϕ0.4 mm, fiber feed rate (V_f) of 3 mm/s, print head movement speed (V_m) of 40 mm/s, and retraction speed (V_r) of 5 mm/s. At a CF-PLA monofilament diameter of ϕ135 µm, the tensile strength and Young's modulus reached maximum values of 48.3 MPa and 2481.8 MPa, respectively. Numerous CF monofilaments (approximately 135 µm in diameter) were observed on the surface and within the CF-PLA boards, significantly enhancing their strength. When the CF content was 4 vol%, the thermal decomposition temperature of the CF-PLA monofilament was 312.53 °C. At 8 vol% CF content, the thermal decomposition temperature increased to 342.62 °C—approximately 30 °C higher than that of the monofilament with 4 vol% CF. The CF-PLA monofilaments fabricated at 8 vol% demonstrated high thermal stability.

Keywords: 3D printing; carbon fiber; polylactic acid; mechanical property; thermal performance

check for updates

Citation: Jin, P.; Pan, T.; Li, Y.; Zhong, T.; Jiang, J.; Pu, C.; Ma, C. Performance and Thermal Properties of 3D Printed CF-Reinforced PLA Monofilaments. *Coatings* **2024**, *14*, 1479. https://doi.org/10.3390/coatings14121479

Academic Editors: Torsten Brezesinski and Tadeusz Hryniewicz

Received: 13 October 2024
Revised: 11 November 2024
Accepted: 19 November 2024
Published: 22 November 2024

Copyright: © 2024 by the authors. Licensee MDPI, Basel, Switzerland. This article is an open access article distributed under the terms and conditions of the Creative Commons Attribution (CC BY) license (https://creativecommons.org/licenses/by/4.0/).

1. Introduction

3D printing technology is a rapid prototyping method that enables the production of complex-shaped parts from filamentous, powdered, or liquid materials [1–3]. Fused melt deposition (FDM) is a type of 3D printing technology known for its fast processing speed, low production cost, and wide range of applications. It is widely used in various fields, including machinery, the chemical industry, and medical treatment [4]. Poly(lactic acid) (PLA) is a specialized thermoplastic material that has become one of the most widely used raw materials due to its desirable properties, including excellent degradability, biocompatibility, low shrinkage, and minimal warpage [5]. However, PLA has relatively low strength and mechanical properties. As a result, some researchers have explored the addition of adding carbon fiber (CF) to PLA to create carbon fiber-reinforced Poly(lactic acid) (denoted as CF-PLA) material. For instance, Xu et al. [6] reported the fabrication of CF-PLA composites via a solution blending and freeze-drying method. Ansari et al. [7] successfully developed CF-PLA materials and found that the Izod impact strength was affected by the printing speed. Lei et al. [8] fabricated CF-PLA boards by using FDM. The results indicated that the carbon fibers in CF-PLA boards were randomly oriented. This highlights the importance of drawing CF-PLA into fibers and aligning the carbon fibers in the direction of the applied

force. Such alignment is essential for enhancing the mechanical properties of CF-PLA monofilaments. The main findings of the literature mentioned above are listed in Table 1. It was found that many studies on CF-PLA materials had been reported by scholars at home and abroad. They mainly studied the effects of the filament feed rate and the print head movement rate on microstructures and performances of CF-PLA composites or laminae. The effects of the print head retraction speed on microstructures and performances of CF-PLA monofilaments and boards have rarely been investigated. Therefore, it is necessary to study these monofilaments and boards, which is of great research significance for the preparation of new parts via 3D printing.

Table 1. Comparison of the related studies for fabricating CF-PLA materials.

References	Products	Preparation Method	Performances
Ref. [6]	CF-PLA-CS (CS: Chitosan) composites	Solution blending and freeze-drying method	Porous biomaterials
Ref. [7]	CF-reinforced PLA composites	3D printing	1. The monofilament diameters in CF-PLA composites are 400–500 μm. 2. The hardness of CF-PLA is 37.95% higher in comparison to pure PLA.
Ref. [8]	PLA/CF lamina	3D printing	1. Establish an accurately micromechanical model that characterizes the true internal microstructure of material. 2. The decrease in Young's modulus in the printed parts of the two deposition configurations caused by the increase in layer thickness reached 8.7% and 18.2%, respectively.

In this study, 3D printing technology was used to draw CF-PLA into monofilaments. The effects of the print head movement speed and retraction rate on the diameter of CF-PLA monofilaments were investigated. The surface morphology and properties were analyzed using scanning electron microscopy (SEM) and thermogravimetric analysis (TGA). CF-PLA monofilaments were also printed into boards with varying CF content, and the mechanical properties of the boards were evaluated. This study provides a valuable insight for crafting high-strength and high-performance components.

2. Experimental Section

2.1. Materials and Preparation

A DF-G3545 3D printer (Zhuhai Dufen Automation Technology Co., Ltd., Zhuhai, China), as shown in Figure 1, was used to fabricate CF-PLA monofilaments. During the 3D printing process, the nozzle diameter was ϕ0.4 mm, the filament feed rate (V_f) was set to 3 mm/s, and the print head movement speed (V_m) ranged from 20 mm/s to 50 mm/s, while the retraction speed (V_r) varied from 0 mm/s to 10 mm/s. The 3D printing parameters are presented in Table 2.

The CF-PLA filament with a diameter of ϕ1.75 mm was purchased from Guangzhou Huicai Material Co., Ltd., Guangzhou, China. The properties of the CF-PLA filament were listed as follows: 1.4%–1.5% refractive index, 175 °C–180 °C melting point, 400–600 kg/mm^2 Young's modulus, 25%–35% break elongation rate, and 18–19 kJ/g combustion heat. It was noted that CF-PLA monofilaments were prepared as follows: (1) Mixing PLA with CF to create CF-PLA powders, and then the CF-PLA powders were squeezed into wires using twin-screw extruder and single-screw extruder. (2) The CF-PLA wires were cooled with water and then pressed into a filament with a diameter of ϕ1.75 mm using a spinning machine. (3) The CF-PLA filament was printed into the CF-PLA board with a size of 100 mm × 20 mm × 5 mm. A schematic diagram of the CF-PLA board fabrication process is presented in Figure 2. It was emphasized that the vol% CF content pertains to the CF

content within the CF-PLA monofilaments, so the CF content change discussed in this work refers to the change in the production of monofilaments. In addition, the number of measurements for the monofilament diameter and the tensile properties should be defined—set at 5 times for each sample. According to the law of conservation of volume [9], the diameter of CF-PLA fiber (D_f) can be estimated via Equation (1).

$$D_f = \sqrt{\frac{\pi V_f}{4V_m}} \quad (1)$$

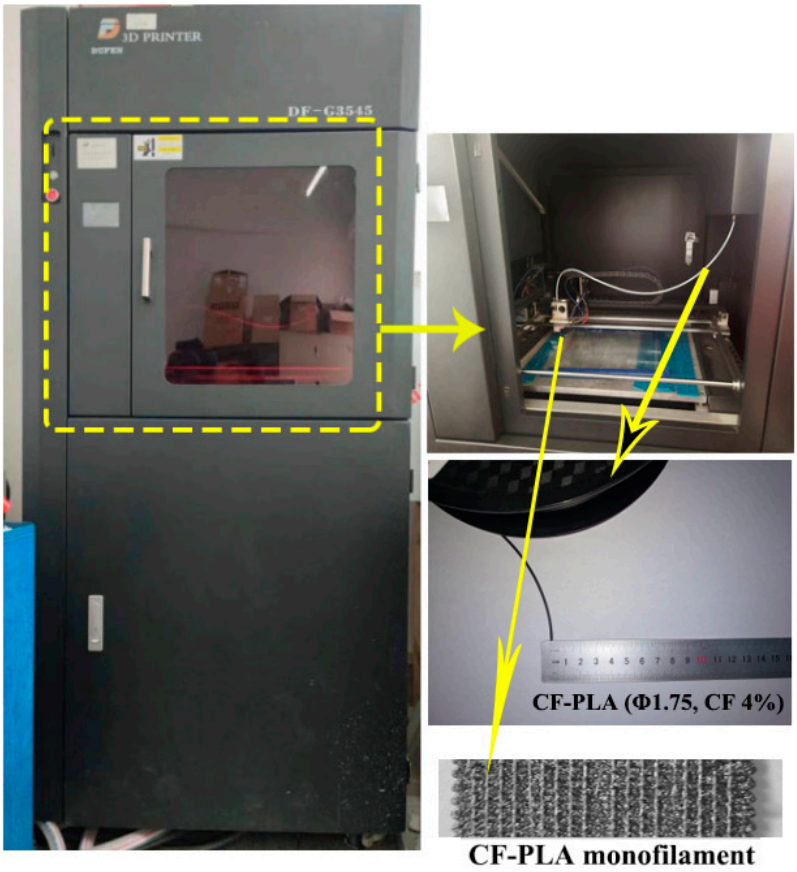


Figure 1. Three-dimensional printer for fabricating CF-PLA monofilaments.

Table 2. Three-dimensional printer system and printing parameters for fabricating CF-PLA monofilaments.

Contents	Parameters
Model	DF-G3545
Printing size (mm)	350 × 350 × 450
Printing accuracy (mm)	±0.05
Filament diameter (mm)	ϕ1.75
Nozzle diameter (mm)	ϕ0.4
Print temperature (°C)	200
Table temperature (°C)	50
Top and bottom line	3
Wall line	3
CAD program	Solidwork2023
Slicer program	Ultimaker Cura5.7

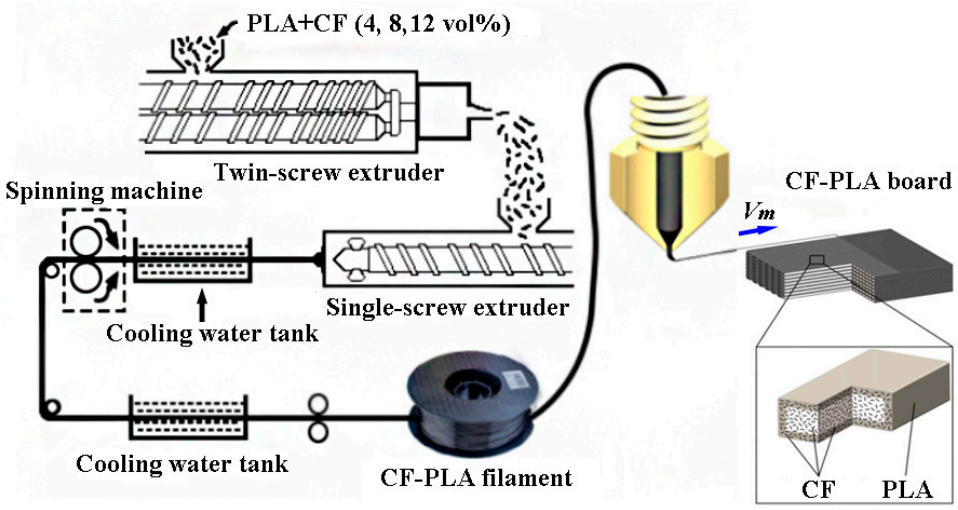


Figure 2. Schematic diagram for fabricating CF-PLA boards.

2.2. Characterization

The surface morphology of CF-PLA monofilaments was observed using a VHX-1000 optical microscope (OM, Beijing Maisiqi High-Tech. Co., Ltd., Beijing, China), while their cross-sectional morphology was investigated with an Apreo20 scanning electron microscope (SEM, Thermo Scientific™ Co., Ltd., Waltham, MA, USA). The CF-PLA monofilaments were first treated with liquid nitrogen to induce brittleness, followed by gold sputtering. Finally, the cross-sectional morphology of the CF-PLA monofilaments was analyzed using SEM.

The mechanical properties of CF-PLA monofilaments and boards were measured using an electronic universal testing machine following the GB9997-1988 standard [10]. The experimental parameters were as follows: the initial fixture distance was set to 20 mm, and the stretching rate was 100 mm/min. The thermal weight analysis of the monofilaments was performed using an X-type thermogravimetric analyzer (HS-TGA-101, Shanghai Hecheng Instrument Technology Co., Ltd., Shanghai, China). The testing conditions were as follows: nitrogen (N_2) was used as the protective gas, the heating rate was 20 °C/min, and the temperature range was scanned from 20 °C to 600 °C.

3. Results and Discussion

3.1. Influence of Retraction Rate on Uniformity of CF-PLA Monofilaments

Figure 3 shows the optical images of CF-PLA monofilaments prepared at different V_r values with a V_m of 40 mm/s. When the V_r was 10 mm/s, the CF-PLA monofilament appeared a broken state (Figure 3a), while the CF-PLA monofilament obtained at 5 mm/s was uniform and compact along the axial direction, as shown in Figure 3b. However, as the V_r value decreased to zero, the diameter of CF-PLA monofilament gradually decreased along the axial direction, and a conical CF-PLA monofilament was formed (Figure 3c).

The explanation is as follows: Due to the viscoelastic nature of CF-PLA monofilament, the pressure exerted by the printing nozzle during the 3D printing process causes the monofilament to deform elastically, leading to the development of internal stress within the material [11]. When the V_r is set to 10 mm/s, the retraction tension exerted by the print head is too strong, causing the CF to break. At a V_r of 0 mm/s, the internal stress within the monofilament gradually releases at a V_m of 40 mm/s, resulting in the formation of a conical CF-PLA monofilament. However, when the V_r is set to 5 mm/s, the retraction force applied by the print head fully relieves the monofilament's internal stress [12], producing a uniform and compact CF-PLA monofilament.

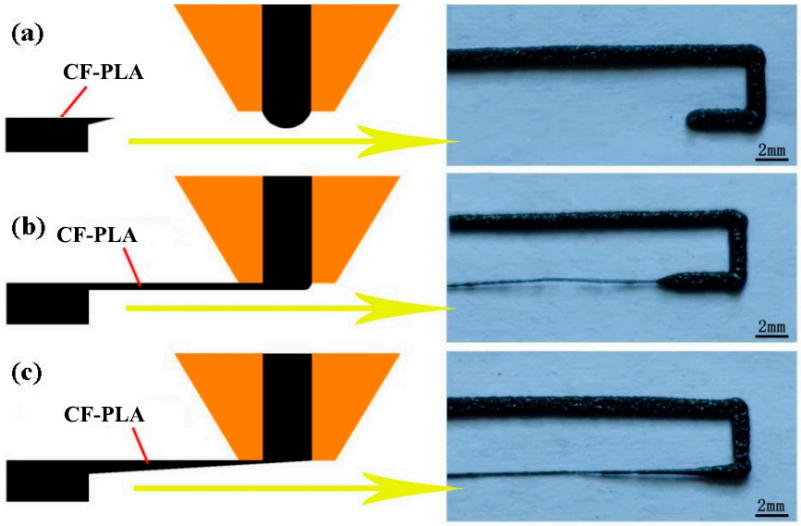


Figure 3. Influence of retraction rates on uniformities of CF-PLA monofilaments: (**a**) V_r = 10 mm/s, (**b**) V_r = 5 mm/s, (**c**) V_r = 0 mm/s.

3.2. Influence of Movement Rate on Diameters of CF-PLA Monofilaments

Figure 4 presents the optical morphologies of CF-PLA monofilaments produced at different V_m values with a constant V_r of 5 mm/s. At a V_m of 20 mm/s, numerous large pits were observed on the monofilament surface, and the fiber had a diameter of ϕ283 µm (Figure 4a). When the V_m was increased to 30 mm/s, small protrusions appeared on the surface, and the diameter decreased to ϕ195 µm (Figure 4b). At a V_m of 40 mm/s, the CF-PLA monofilament exhibited a uniform diameter and a smooth surface, with a diameter of ϕ135 µm (Figure 4c). However, at a V_m of 50 mm/s, the monofilament diameter (ϕ75 µm) varied significantly, resulting in uneven diameters across small sections.

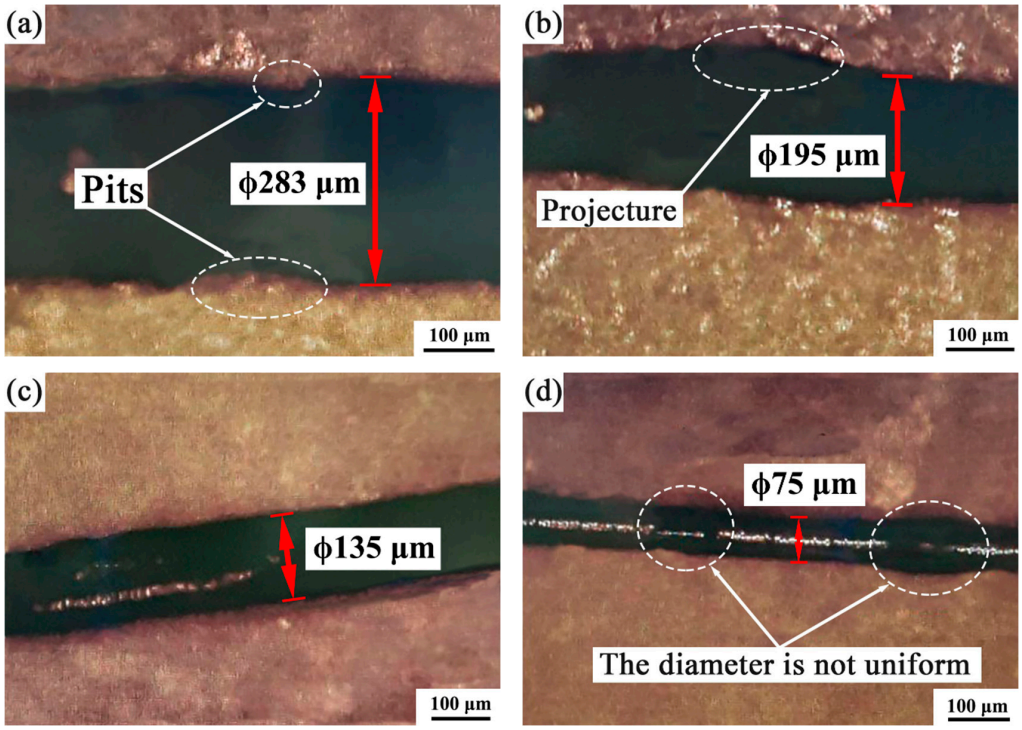


Figure 4. Optical microscope images of CF-PLA monofilaments prepared at different print head movement rates: (**a**) V_m = 20 mm/s, (**b**) V_m = 30 mm/s, (**c**) V_m = 40 mm/s, (**d**) V_m = 50 mm/s.

This occurs because, as the V_m value increases, the carbon fibers within the CF-PLA monofilaments tend to become more aligned [13]. At V_m values of 20 mm/s and 30 mm/s, the carbon fibers are unevenly distributed, leading to the formation of pits and protrusions on the monofilament surface. When the V_m reaches 40 mm/s, the carbon fibers become better aligned, resulting in a smooth and compact structure. However, at a V_m of 50 mm/s, the cooling rate increases as the monofilament diameter decreases, reducing the flowability of the CF-PLA material. This results in inconsistent monofilament diameters.

3.3. Analysis of Cross-Sectional Morphologies

Figure 5 presents the cross-sectional microstructures of CF-PLA monofilaments produced at different V_r values. When the *Vr* was 10 mm/s, many CF fibers broke off. The print head moved too quickly, generating excessive shear force on the fibers, which caused many CF fibers to break (Figure 5a). However, when the V_r value was set to 5 mm/s, the CF fibers aligned orderly along the axial direction (Figure 5b). At this optimal V_r value, the nozzle applied higher shear stress to the fibers, causing the CFs to rotate in the print direction [14]. As a result, many CF fibers became aligned parallel to the CF-PLA monofilaments. When zero retraction was applied during 3D printing, some CFs broke due to a reduction in the CF-PLA monofilament diameter.

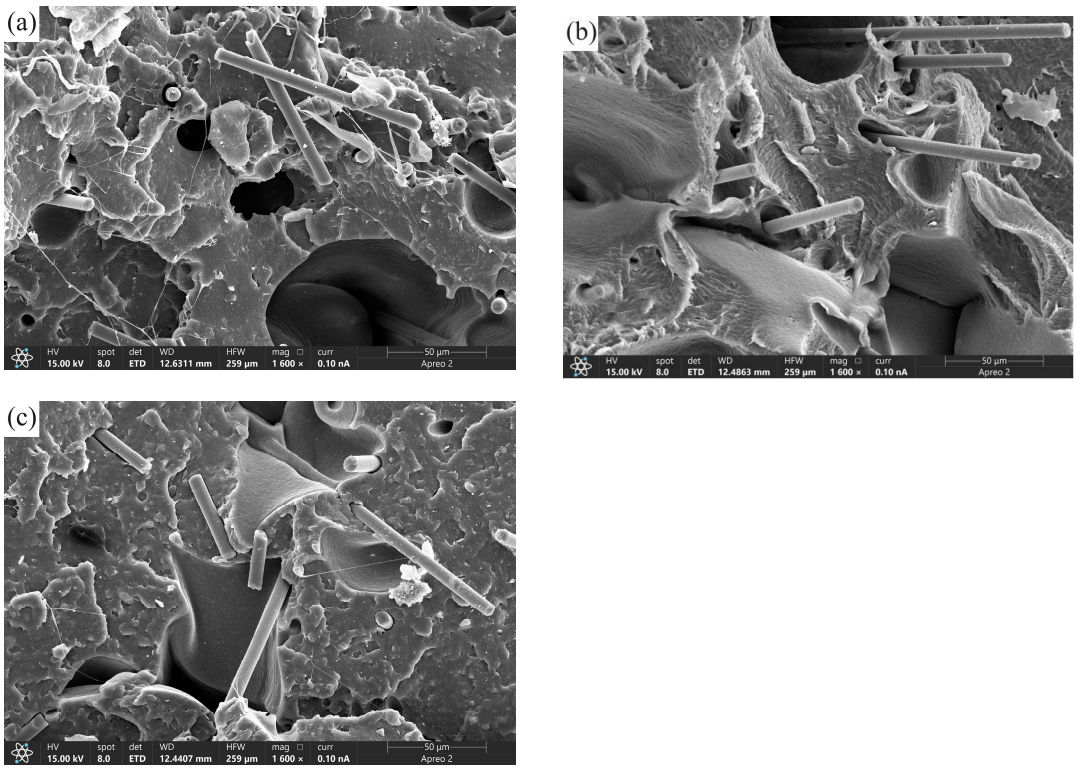


Figure 5. SEM images of CF-PLA monofilaments produced at: (**a**) V_r = 10 mm/s, (**b**) V_r = 5 mm/s, (**c**) V_r = 0 mm/s.

3.4. Mechanical Properties of CF-PLA Monofilaments

3.4.1. Tensile Strength and Young's Modulus of CF-PLA Monofilaments

Figure 6 shows the tensile strength and Young's modulus of CF-PLA monofilaments (8 vol% CF content) with varying diameters. As the monofilament diameter increased from ϕ75 μm to ϕ135 μm, both tensile strength and Young's modulus also increased. At a diameter of ϕ135 μm, the CF-PLA monofilaments reached their maximum tensile strength of 48.3 MPa and Young's modulus of 2481.8 MPa. This improvement is due to the increased number of CF fibers aligned along the axis as the monofilament diameter grows. When subjected to tensile forces, more CF fibers bear the load along the axis, thereby enhancing

the mechanical properties of the CF-PLA monofilaments [15,16]. However, when the diameter of the CF-PLA monofilaments exceeded ϕ135 μm, both its tensile strength and Young's modulus began to decline. This decrease is primarily due to the aggregation of CF fibers within the CF-PLA monofilaments, which negatively impacts its mechanical properties [17].

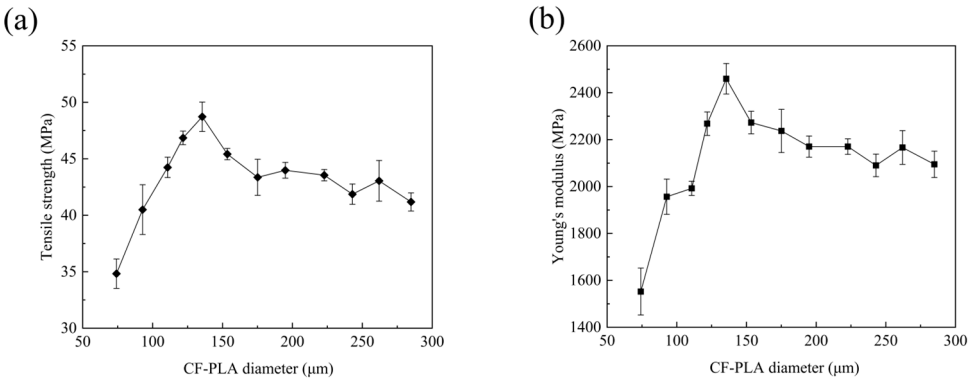


Figure 6. (**a**) Tensile strength and (**b**) Young's modulus of CF-PLA monofilaments produced at different diameters.

3.4.2. Properties of Boards Fabricated from Monofilaments

Figure 7 shows the physical appearance of boards 3D-printed using PLA and CF-PLA monofilaments (8 vol% CF content), while Figure 8 displays their tensile strength and Young's modulus. Both boards measured 100 mm × 20 mm × 5 mm, and the main printing parameters for producing PLA and CF-PLA boards were listed as follows: (1) PLA board: V_f of 3 mm/s, V_m of 40 mm/s, and V_r of 5 mm/s. (2) CF-PLA board: 8 vol% CF content, V_f of 3 mm/s, V_m of 40 mm/s, and V_r of 5 mm/s. It was noted that the boards printed from PLA with and without CF were obtained in the same way.

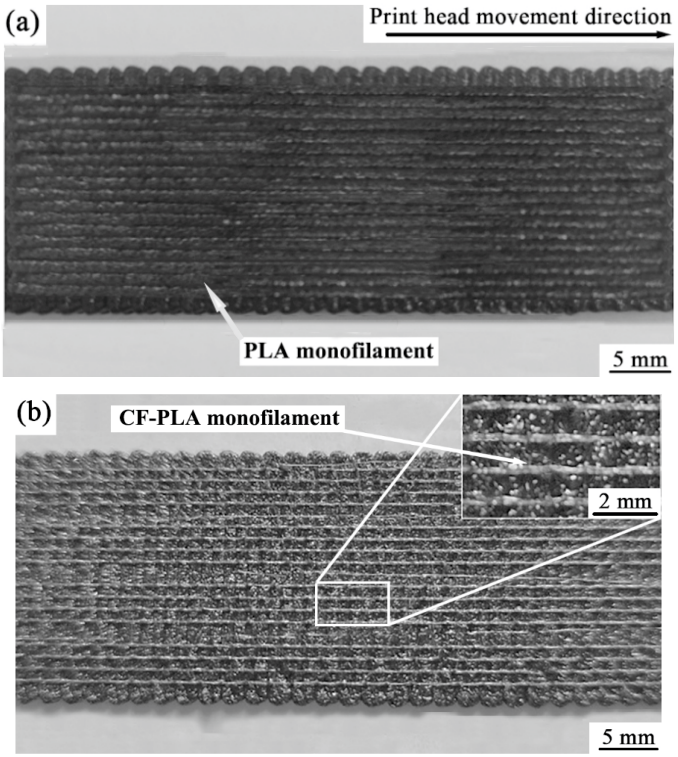


Figure 7. Physical picture of the boards 3D-printed by using (**a**) PLA and (**b**) CF-PLA monofilaments (8 vol% CF).

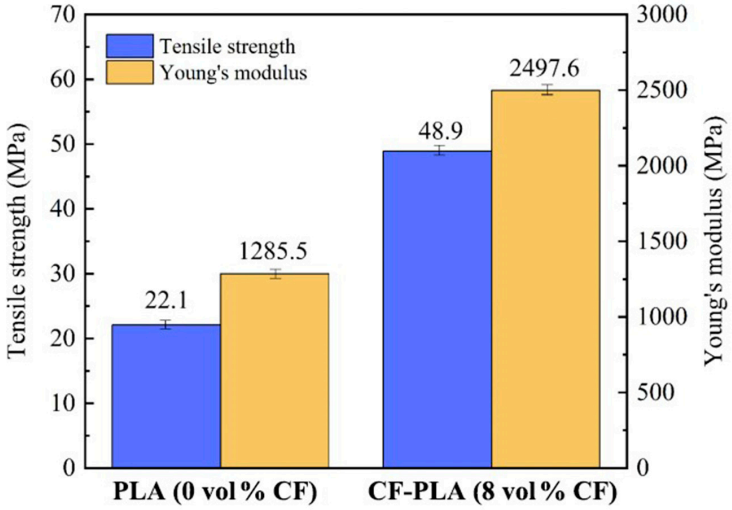


Figure 8. Tensile strength and Young's modulus of the monofilaments.

The PLA board exhibited numerous fusion interfaces, significantly weakening its properties (Figure 7a), with a tensile strength of 22.1 MPa and a Young's modulus of 1285.5 MPa. In contrast, the CF-PLA board featured numerous CF fibers (~135 μm in diameter) both on the surface and within the material (Figure 7b), significantly enhancing its strength. The tensile strength and Young's modulus of the CF-PLA board were 48.9 MPa and 2497.6 MPa, respectively.

3.4.3. Effect of CF Content on Properties of CF-PLA Monofilaments

To examine the mechanical properties of the CF-PLA monofilaments, we devised CF-PLA monofilaments through blending PLA and CF in various proportions (100:0, 96:4, 92:8, 88:12). The CF contents in the CF-PLA monofilaments were 0 vol%, 4 vol%, 8 vol%, and 12 vol%, respectively. Figure 9 illustrates the effect of CF content on the tensile strength and Young's modulus of the CF-PLA monofilaments. As the CF content increased from 0 vol% to 8 vol%, both tensile strength and Young's modulus of the monofilaments showed a gradual rise. At CF content equivalent to 8 vol%, the monofilaments exhibited the highest tensile strength and Young's modulus, approximately 2.5 times greater than those of PLA monofilaments. This improvement is due to the increased number of CF fibers, which enhances the mechanical properties of the CF-PLA monofilaments [18]. However, when the CF content increased from 8 vol% to 12 vol%, both the tensile strength and Young's modulus began to decline. This is because, at higher CF content, the distance between CF fibers decreases, making them more prone to breaking during 3D printing, as shown in Figure 10, leading to reduced mechanical strength and stiffness.

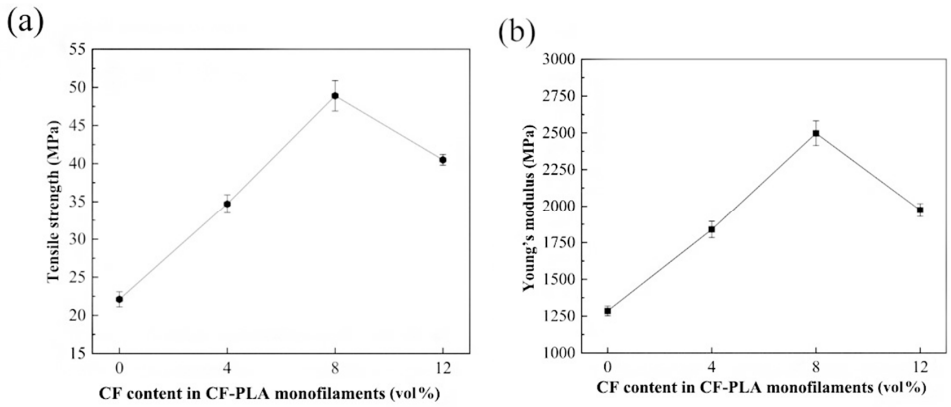


Figure 9. Effect of CF content on (**a**) tensile strength and (**b**) Young's modulus of CF-PLA monofilaments.

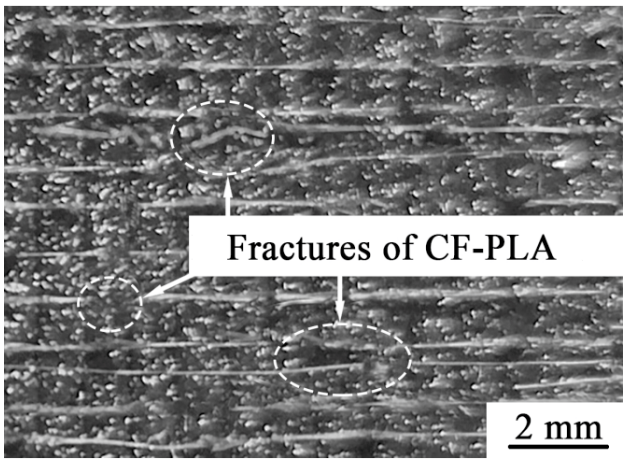


Figure 10. SEM image of the CF-PLA monofilament produced at 12 vol%.

3.5. Thermal Properties of CF-PLA Monofilaments

To detect the thermal properties of CF-PLA monofilaments, we also fabricated CF-PLA monofilaments through mixing PLA and CF in various proportions of 100:0, 96:4, 92:8, and 88:12. Then, the CF-PLA monofilaments with CF contents of 0 vol%, 4 vol%, 8 vol%, and 12 vol% were produced by using 3D printing technology. Figure 11 presents the thermogravimetric curves of the CF-PLA monofilaments at different CF contents. When the CF content was 4 vol%, the thermal decomposition temperature of the CF-PLA monofilament was 312.53 °C. At 8 vol% CF content, the thermal decomposition temperature increased to 342.62 °C, approximately 30 °C higher than that of the monofilament with 4 vol% CF. However, the thermal decomposition temperature decreased slightly to 334.55 °C when the CF content was 12 vol%. These results suggest that the thermal decomposition temperature increases with higher CF content, reaching its maximum at 8 vol% CF content.

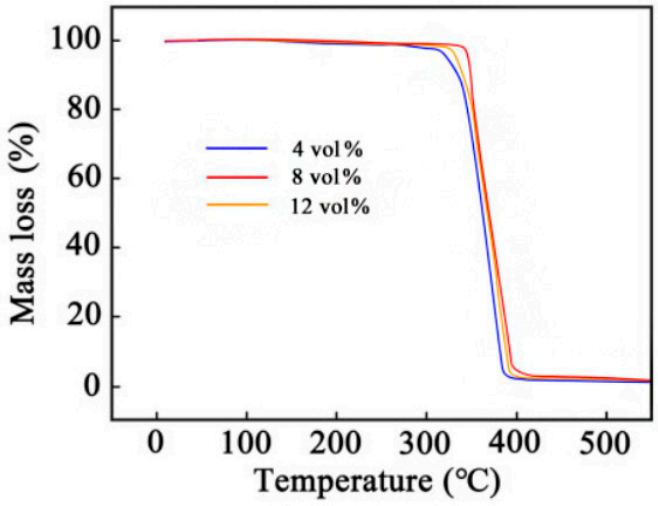


Figure 11. Thermogravimetric curves of CF-PLA monofilaments produced at different CF contents.

Figure 12 shows the derivative thermogravimetry curves of the CF-PLA monofilaments with varying CF contents. The mass loss peaks of the monofilaments corresponded to different thermal decomposition temperatures. For monofilaments with CF contents of 4 vol%, 8 vol%, and 12 vol%, the mass loss peaks occurred at 366.3 °C, 378.4 °C, and 372.5 °C, respectively. These results indicate that the CF-PLA monofilament with 8 vol% CF content exhibited the highest thermal stability.

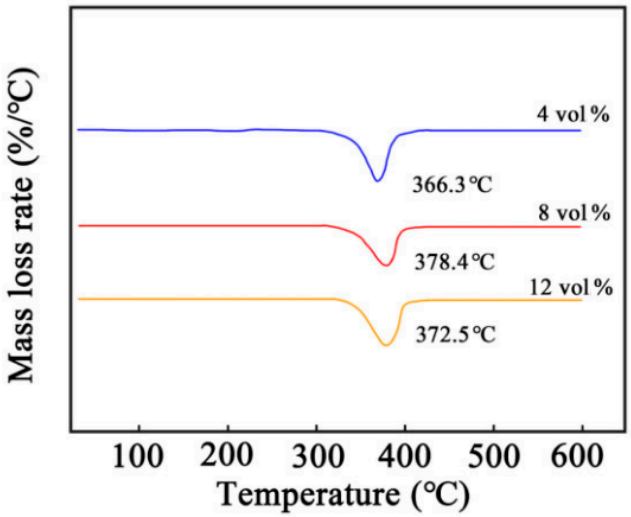


Figure 12. Derivative thermogravimetry curves of CF-PLA monofilaments produced at different CF contents.

The underlying reason for this phenomenon is that the thermal conductivity of the CF-PLA monofilament is higher than that of the PLA monofilament. As the CF content increases, the CF-PLA monofilament can withstand higher temperatures before decomposing [19,20]. As a result, the thermal stability of the CF-PLA monofilaments is enhanced. However, when the CF content becomes too high, it causes internal stress concentration within the monofilaments, and then more cracks formed in CF-PLA monofilaments, leading to a reduction in their thermal stability [21].

4. Conclusions

1. During 3D printed CF-PLA monofilaments, the optimal printing parameters were a nozzle diameter of ϕ0.4 mm, fiber feed rate (V_f) of 3 mm/s, print head movement speed (V_m) of 40 mm/s, and a retraction speed (V_r) of 5 mm/s.
2. At a CF-PLA monofilament diameter of ϕ135 μm, the tensile strength and Young's modulus reached maximum values of 48.3 MPa and 2481.8 MPa, respectively. At a CF content equivalent to 8 vol%, the monofilaments exhibited the highest tensile strength and Young's modulus—approximately 2.5 times greater than those of PLA monofilaments.
3. When the CF content was 4 vol%, the thermal decomposition temperature of the CF-PLA monofilament was 312.53 °C. At 8 vol% CF content, the thermal decomposition temperature increased to 342.62 °C—approximately 30 °C higher than that of the monofilament with 4 vol% CF. The CF-PLA monofilaments fabricated at 8 vol% demonstrated high thermal stability.

Author Contributions: Conceptualization and methodology, P.J.; software and methodology, T.P.; validation and formal analysis, Y.L.; conceptualization and investigation, T.Z.; investigation and resources, J.J.; data curation and resources, C.P.; writing—original draft, C.M. All authors have read and agreed to the published version of the manuscript.

Funding: This study was supported by the Gansu Provincial Science and Technology Plan-Key R&D Program Project (No. 23YFGA0073), the Lanzhou City Science and Technology Plan Project (No. 2023-3-76), and the Fundamental Research Funds for the Central Universities (No. 31920230143).

Institutional Review Board Statement: Not applicable.

Informed Consent Statement: Not applicable.

Data Availability Statement: Data are contained within the article.

Conflicts of Interest: The authors declare no conflicts of interest.

References

1. Singh, S.; Singh, M.; Prakash, C.; Gupta, M.K.; Mia, M.; Singh, R. Optimization and Reliability Analysis to Improve Surface Quality and Mechanical Characteristics of Heat-Treated Fused Filament Fabricated Parts. *Int. J. Adv. Manuf. Technol.* **2019**, *102*, 1521–1536. [CrossRef]
2. Tüfekci, K.; Çakan, B.G.; Küçükakarsu, V.M. Stress Relaxation of 3D Printed PLA of Various Infill Orientations under Tensile and Bending Loadings. *J. Appl. Polym. Sci.* **2023**, *140*, e54463. [CrossRef]
3. Prajapati, A.R.; Dave, H.K.; Raval, H.K. Effect of Fiber Volume Fraction on the Impact Strength of Fiber Reinforced Polymer Composites Made by FDM Process. *Mater. Today Proc.* **2021**, *44*, 2102–2106. [CrossRef]
4. Tutar, M. A Comparative Evaluation of the Effects of Manufacturing Parameters on Mechanical Properties of Additively Manufactured PA and CF-Reinforced PA Materials. *Polymers* **2023**, *15*, 38. [CrossRef] [PubMed]
5. Tunçel, O. Optimization of Charpy Impact Strength of Tough PLA Samples Produced by 3D Printing Using the Taguchi Method. *Polymers* **2024**, *16*, 459. [CrossRef] [PubMed]
6. Xu, W.F. Evaluation of Cell Compatibility for Porous 3D CF/PLA/CS Composites Scaffold In Vitro. *Chin. J. Appl. Chem.* **2011**, *28*, 214–218. (In Chinese)
7. Ansari, A.A.; Kamil, M. Izod impact and hardness properties of 3D printed lightweight CF-reinforced PLA composites using design of experiment. *Int. J. Lightweight Mater. Manuf.* **2022**, *5*, 369–383. [CrossRef]
8. Lei, M.; Wang, Y.; Wei, J.W.Y. Micromechanical modeling and numerical homogenization calculation of effective stiffness of 3D printing PLA/CF composites. *J. Manuf. Process.* **2023**, *102*, 37–49. [CrossRef]
9. Zhang, Z.; Li, M.; Wang, Y.; Dai, W.; Li, L.; Chen, Y.; Kong, X.; Xu, K.; Yang, R.; Gong, P.; et al. Ultrahigh thermal conductive polymer composites by the 3D printing induced vertical alignment of carbon fiber. *J. Mater. Chem. A* **2023**, *11*, 10971–10983. [CrossRef]
10. *GB/T 9997-1988*; Man-Made Fibres—Determination of Breaking Strength and Elongation of Individual Fibres. China National Textile Industry Federation: Beijing, China, 1988.
11. Gantenbein, S.; Mascolo, C.; Houriet, C.; Zboray, R.; Neels, A.; Masania, K.; Studart, A. Spin-Printing of Liquid Crystal Polymer into Recyclable and Strong All-Fiber Materials. *Adv. Funct. Mater.* **2021**, *31*, 2104574. [CrossRef]
12. Hivet, G.; Vidal-Sallé, E.; Boisse, P. Analysis of the stress components during the forming of a textile composite reinforcement. *Key Eng. Mater.* **2013**, *554–557*, 492–500. [CrossRef]
13. Symes, M.D.; Kitson, P.J.; Yan, J.; Richmond, C.J.; Cooper, G.J.T.; Bowman, R.W.; Vilbrandt, T.; Cronin, L. Integrated 3D-printed reactionware for chemical synthesis and analysis. *Nat. Chem.* **2012**, *4*, 349–354. [CrossRef]
14. Luo, H.; Xiong, G.; Ma, C.; Chang, P.; Yao, F.; Zhu, Y.; Zhang, C.; Wan, Y. Mechanical and thermo-mechanical behaviors of sizing-treated corn fiber/polylactide composites. *Polym. Test.* **2014**, *39*, 45–52. [CrossRef]
15. Shen, L.; Yang, H.; Ying, J.; Qiao, F.; Mao, P. Preparation and mechanical properties of carbon fiber reinforced hydroxyapatite/polylactide biocomposites. *J. Mater. Sci. Mater. Med.* **2007**, *20*, 2259–2265. [CrossRef] [PubMed]
16. Xia, F.; Yan, P.; Ma, C.; Wang, B.; Liu, Y. Effect of different heat-treated temperatures upon structural and abrasive performance of Ni-TiN composite nanocoatings. *J. Mater. Res. Technol.* **2023**, *27*, 2874–2881. [CrossRef]
17. Pandey, D.; Pandey, R.; Mishra, A.; Tewari, R.P. Effect of Printing Temperature on Fatigue and Impact Performance of 3-D Printed Carbon Fiber Reinforced PLA Composites for Ankle Foot Orthotic Device. *Mech. Compos. Mater.* **2024**, *60*, 549–560. [CrossRef]
18. Mahesh, S.; Beyerlein, I.J.; Phoenix, S.L. Size and heterogeneity effects on the strength of fibrous composites. *Phys. D Nonlinear Phenom.* **1999**, *133*, 371–389. [CrossRef]
19. Keith, J.M.; King, J.A.; Miller, M.G.; Tomson, A.M. Thermal conductivity of carbon fiber/liquid crystal polymer composites. *J. Appl. Polym. Sci.* **2006**, *102*, 5456–5462. [CrossRef]
20. Hasdiansah, H.; Yaqin, R.I.; Pristiansyah, P.; Umar, M.L.; Priyambodo, B.H. FDM-3D Printing Parameter Optimization Using Taguchi Approach on Surface Roughness of Thermoplastic Polyurethane Parts. *Int. J. Interact. Des. Manuf.* **2023**, *17*, 3011–3024. [CrossRef]
21. Fan, W.; Li, J.; Zheng, Y.; Liu, T.; Tian, X.; Sun, R. Influence of thermo-oxidative aging on the thermal conductivity of carbon fiber fabric reinforced epoxy composites. *Polym. Degrad. Stab.* **2016**, *123*, 162–169. [CrossRef]

Disclaimer/Publisher's Note: The statements, opinions and data contained in all publications are solely those of the individual author(s) and contributor(s) and not of MDPI and/or the editor(s). MDPI and/or the editor(s) disclaim responsibility for any injury to people or property resulting from any ideas, methods, instructions or products referred to in the content.